



## Qualitative and quantitative discrimination of fake and true alkene rotation processes in pd( $\eta^2$ -olefin) complexes. A new bimolecular mechanism

Vittorio Lucchini<sup>a,\*</sup>, Giuseppe Borsato<sup>a</sup>, Luciano Canovese<sup>b,\*</sup>, Claudio Santo<sup>b</sup>, Fabiano Visentin<sup>b</sup>, Alfonso Zambon<sup>a</sup>

<sup>a</sup>Dipartimento di Scienze Ambientali, Università Ca' Foscari di Venezia, Dorsoduro 2137, I-30123 Venezia, Italy

<sup>b</sup>Dipartimento di Chimica, Università Ca' Foscari di Venezia, Dorsoduro 2137, I-30123 Venezia, Italy

### ARTICLE INFO

#### Article history:

Received 15 October 2008

Received in revised form 1 December 2008

Accepted 8 December 2008

Available online 25 December 2008

#### Keywords:

Pd( $\eta^2$ -olefin) complexes

Mechanisms of fluxional behaviour

Alkene rotation

### ABSTRACT

The fluxional behaviour of  $[Pd(\eta^2-fn)(N-SMe)]$  (**2**) (*fn* = fumaronitrile, N-SMe = 2-methylthiomethylpyridine) and of  $[Pd(\eta^2-tmetc)(N-N'-4-anisyl)]$  (**3**) (*tmetc* = tetramethylethylenetetracarboxylate, *N-N'*-4-anisyl = 2-(4-methoxyphenyliminomethane)pyridine) were monitored by  $^1H$  NMR spectroscopy and quantitatively determined by line-shape analyses (for **2**) and selective inversion recovery experiments (for **3**). The coalescence of the AB multiplet of *fn* hydrogens of **2** is concentration dependent and presents a strongly negative  $\Delta S^\ddagger$ , suggesting the intermediacy of a dimeric complex and ruling out the hypothesis of olefin rotation. The accurate evaluation of all spectral features also allows determination of the approaching mode of the monomeric units. The inversion transfer between the *tmetc* methyls of **3** reveals a true propeller-like olefin rotation. The presence of a nucleophilic electron pair at sulfur in **2** triggers the formation of the dimeric intermediate.

© 2008 Elsevier B.V. All rights reserved.

### 1. Introduction

Many transition-metal  $\pi$ -complexes with unsaturated organic substrates present fluxional behaviour with a time scale compatible with detection and measurement by NMR techniques. The complexes of Pd with olefins  $[Pd(\eta^2\text{-olefin})(L-L')]$  (but also the complexes of Pt or Rh) present  $^1H$  NMR olefinic signals corresponding to hydrogens or other groups which are made non equivalent by the asymmetry of the ancillary L-L' ligand. Their fluxional properties can be analyzed for quantitative information by the techniques of line-shape simulation, bidimensional EXSY spectroscopy, or selective saturation or inversion transfer.

Many molecular movements can account for the temperature averaging or magnetization transfer among olefinic signals. Of these, the least relevant are those within the ancillary ligand L-L', associated with a reduction of asymmetry.

The molecular rearrangements, which imply a variation of the bonds between the central metal atom and the ancillary ligand or the olefin, are more important. The following mechanisms have been considered for the fluxional movements in olefin complexes of Pd, Pt and Rh:

1. the propeller-like olefin rotation. This is the earliest and most frequently proposed mechanism [1–5];
2. olefin-metal dissociation followed by recombination; [3];

3. intermolecular associative process with free alkene, via the intermediation of a  $[M(\eta^2\text{-olefin})_2(L-L')]$  complex [3,5];
4. metal-L or metal-L' bond dissociation, followed by rotation of the ancillary ligand and recombination [4];
5. intermolecular exchange with the free ancillary ligand L-L'. In this case, a mechanism has been proposed which involves an olefin-metal dissociation step [3]. During our investigation [6] of the fluxional behaviour in  $CD_2Cl_2$  of the complex  $[Pd(\eta^2\text{-tmetc})(N-SMe)]$  (**1**) (*tmetc* = tetramethylethylenetetracarboxylate, N-SMe = 2-methylthiomethylpyridine), we discovered a concentration dependent scrambling of the olefin resonances, which could be rationalized only by invoking one further mechanism;
6. bimolecular process through a dimeric complex (see Chart 1).

We verified that the concentration dependence could not be attributed to the action of adventitious free olefin (the addition of *tmetc* did not alter the rearrangement rate) or free ancillary ligand (the addition of N-SMe does indeed accelerate the rearrangement rate; however we could not find any hint for the presence of the free ligand from a careful inspection of the low temperature  $^1H$  NMR spectrum). These observations would rule out the associative mechanisms 3 and 5.

We proposed that the presence of a trivalent sulfur atom, with a residual metallophilic lone pair, is the trigger for the process. Thus the occurrence of this mechanism is dependent on the nature of the ancillary ligand rather than on that of the olefin.

\* Corresponding authors.

E-mail address: cano@unive.it (L. Canovese).

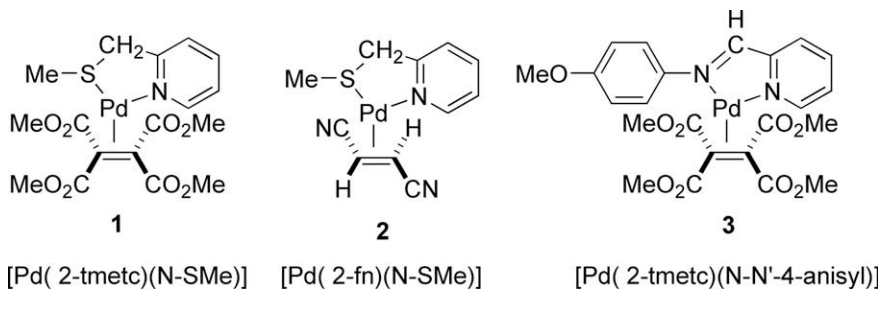


Chart 1.

In order to verify the generality of the mechanism and of the conditions thereof, we undertook the full quantitative analysis of the fluxional behaviour of  $[Pd(\eta^2\text{-fn})(N\text{-SMe})]$  (**2**) (fn = fumaronitrile) (with the same ancillary ligand as **1** but with a different olefin) [7] and of  $[Pd((\eta^2\text{-tmetc})(N\text{-N}'\text{-4-anisyl})]$  (**3**) ( $N\text{-N}'\text{-4-anisyl} = 2\text{-}(4\text{-methoxyphenyliminomethane})\text{pyridine}$ ) (with the same olefin as **1** but with a different ancillary ligand, deprived of any triggering lone pair) [8].

## 2. Results

### 2.1. Dynamic behaviour of $[Pd(\eta^2\text{-fn})(N\text{-SMe})]$ (**2**)

The  $^1\text{H}$  NMR spectra of **2** at increasing temperatures are shown in Fig. 1. The combination of chirality at trigonal sulfur (when the S-methyl orientation is ‘frozen’) and of axial chirality at the olefin-Pd bond gives rise to two diastereoisomers, *l*-**2** (with enantiomers (*Re,R*)-**2** and (*Si,S*)-**2**) and *u*-**2** (with enantiomers (*Re,S*)-**2** and (*Si,R*)-**2**) [9].

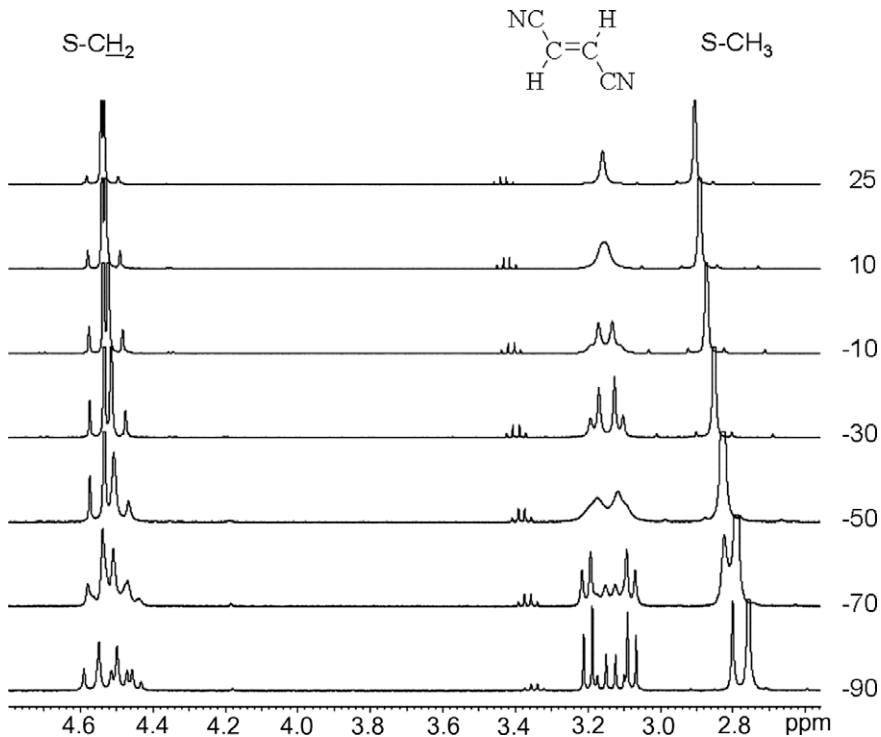
As a matter of fact, at low temperature ( $-90^\circ\text{C}$ , in  $\text{CD}_2\text{Cl}_2$ ) the inversion at sulfur is almost ‘frozen’ at the NMR time scale, and two distinct AB systems, assigned to olefin protons and to the S-

$\text{CH}_2$  methylenic protons, are observed for each diastereoisomer. At this temperature however, the interconversion between the isomers, though not yet manifest in the NMR spectrum, is starting to take place and invalidates any structural determination of *l*-**2** and *u*-**2** by the monitoring of NOEs. Even if the complete structural and spectral assignments are not completely assignable in the case of the present investigation, it is tempting however to attribute the major isomer to *l*-**2**, where S-Me is eclipsed with one fn hydrogen, and the minor one to *u*-**2**, where it is eclipsed with one fn CN. The ab initio optimizations of the structures of *l*-**2** and *u*-**2** confirm this stability order [10]. More on this point in Section 3.

Starting from  $-90^\circ\text{C}$  and with rising temperature, the fn AB systems on one side, and the S- $\text{CH}_2$  AB systems on the other, show the usual dynamic behaviour: line broadening, coalescence to a unique AB system, and final line sharpening.

The merged AB pattern of the S- $\text{CH}_2$  system is maintained at all temperatures above the coalescence temperature: it manifests a more pronounced second order pattern (because of decreasing  $\Delta v$ ) but no sign of line broadening. This persistency must be taken into account in any proposed mechanism.

The two fn AB systems of *l*-**2** and *u*-**2** coalesce at about  $-50^\circ\text{C}$ . There follows a sharpening of the unique AB system up to about

Fig. 1. Aliphatic and vinylic regions of the  $^1\text{H}$  NMR spectra of **2** at selected temperatures.

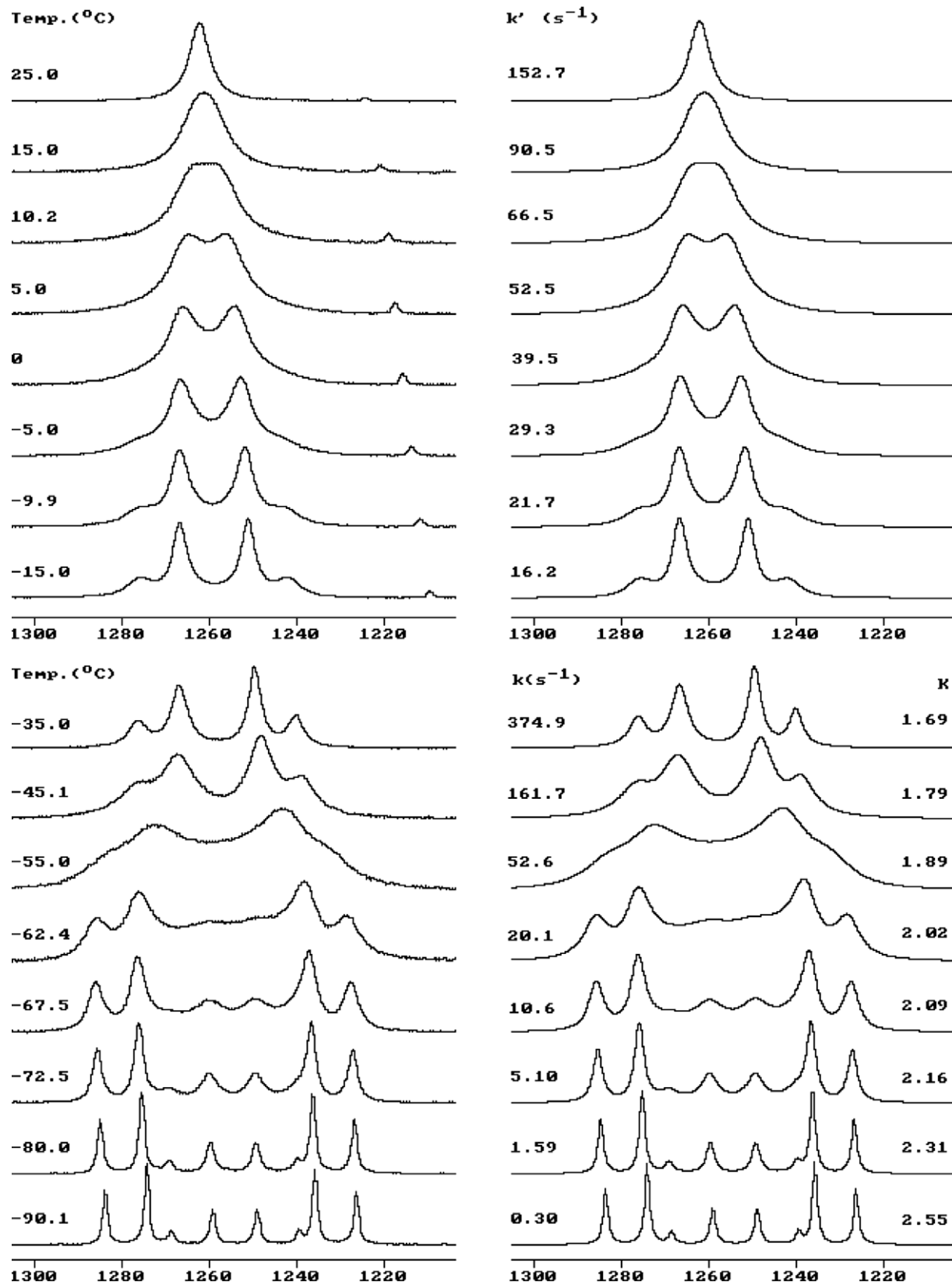


**Fig. 2.** Experimental (left) and simulated (right) spectra of fn hydrogens of **2** in  $\text{CD}_2\text{Cl}_2$  at selected temperatures. From  $-90.1$  to  $-35.0^\circ\text{C}$ : the first order  $k$  kinetic constants and the  $K$  equilibrium constants are calculated on the basis of the exchange scheme  $(\text{AB})_{\text{M}} = (\text{AB})_{\text{m}}$  ( $\text{M}$  major and  $\text{m}$  minor isomer). From  $-15$  to  $25^\circ\text{C}$ : the pseudo first order  $k$  kinetic constants are calculated from the scheme  $\text{AB} = \text{BA}$ . The concentration of **2** is  $9.0 \times 10^{-3} \text{ mol dm}^{-3}$ .

$-35^\circ\text{C}$ . Then (in a sample  $9.0 \times 10^{-3}$  molar) a further broadening, coalescence and final sharpening to a single line show up. Quite

clearly, the high temperature process must be different from that observed at low temperature.

We will show that the low temperature behaviour of the fn and S-CH<sub>2</sub> systems reveal the same molecular process: the inversion at sulfur. The fast inversion at this centre on the NMR time scale will nullify its chiral characteristics, so that we are left, as for NMR, with a pair of enantiomers, *Re*-**2** and *Si*-**2**, and a single set of signals.

## 2.2. Inversion at sulfur

We have performed full line-shape simulation of the coalescing multiplets with the DNMR5 program [11].

The simulation gives as output the kinetic *k* and equilibrium *K* constants, the involved *v* chemical shifts and *J* coupling constants, and the natural line widths expressed as *T*<sub>2</sub> relaxation times. All these quantities are to some degree covariant in the coalescence region, so that different combinations of their magnitudes may result in the same simulated shape. It is customary, but not correct, to assume for the coalescence region the  $\Delta v$ , *J* and *T*<sub>2</sub> values measured in the low temperature region. The parameters  $\Delta v$  and *T*<sub>2</sub> do actually vary with temperature, while the parameter *J* is essentially invariant. Fortunately, the variations of *v* and *T*<sub>2</sub> in the low temperature region are to a good degree linear against 1/*T*, and correct values for the coalescence region (and beyond) may be safely extrapolated (see Supplementary material) [12].

The fn and the S-CH<sub>2</sub> systems are simulated on the basis of the exchange scheme (AB)<sub>M</sub> = (AB)<sub>m</sub>, where M and m indicate the more and the less stable diastereoisomer, either *l*-**2** or *u*-**2**. Fig. 2 documents the accuracy of the simulation for the fn system and for selected temperatures.

The results from the Arrhenius plot of the equilibrium constants *K* and from the Eyring plot of the kinetic constants *k* are reported in Table 1. The equilibrium and activation enthalpies for the two simulated systems are to be considered equal within the statistical error. The corresponding entropies differ somewhat but, because of the intrinsically great errors in their evaluation (obtained from the intercept, and therefore from a long extrapolation, of the Arrhenius or Eyring plots), they are customarily considered if their absolute value is greater than 5 cal mol<sup>-1</sup> K<sup>-1</sup>.

The equality of the results implies that the coalescences of the two fn and S-CH<sub>2</sub> systems reveal the same process. The similarity

with the literature results for **1** [6], also reported in Table 1, suggests that the same process is operative for both complexes. The process is the inversion at sulfur and will be dealt with in the discussion.

## 2.3. Olefin rotation or pseudo rotation

The coalescence of the merged fn system could be analyzed with the DNMR5 program as an AB = BA exchange, at temperatures of -15 °C and above, where the (AB)<sub>M</sub> = (AB)<sub>m</sub> process is too fast to interfere. In the temperature region above -35 and below -15 °C, both processes are significant, and the spectra could not be analyzed.

The parameters of the kinetic constants from the Eyring plot are collected in Table 1, together with the corresponding parameters for complex **1**. The activation entropy displays a negative value well above 5 cal mol<sup>-1</sup> K<sup>-1</sup> which can be traced back to an intermediate or a transition state more ordered with respect to the ground state.

It is tempting to associate this situation to the formation of an ordered dimer [13]. We therefore performed a series of experiments at constant temperature (19 °C) and different concentrations: the AB system shows a coalescence to a singlet with increasing concentration. The concentration dependence of the reaction rates as deduced from line-shape analysis is a clear indication that the reaction under study is a second order process. A similar correlation was reported for **1** [6], and it is also shown in Fig. 3.

Thus the AB = BA process is definitely second order in **2** (and **1**). The linear correlation parameters are given in Table 2. The slopes are the second order kinetic constants at the given temperature. The intercepts are statistically significant and will be commented on in the discussion.

## 2.4. Dynamic behaviour of [Pd(*n*<sup>2</sup>-tmetc)(N-N'-4-anisyl)] (**3**)

The spectrum of **3** in CDCl<sub>3</sub> is still 'frozen' at room temperature, displaying two distinct and sharp resonances for the methyl protons of tmetc. Only at 65 °C do the resonances show an incipient broadening, which is however not sufficient for a fruitful

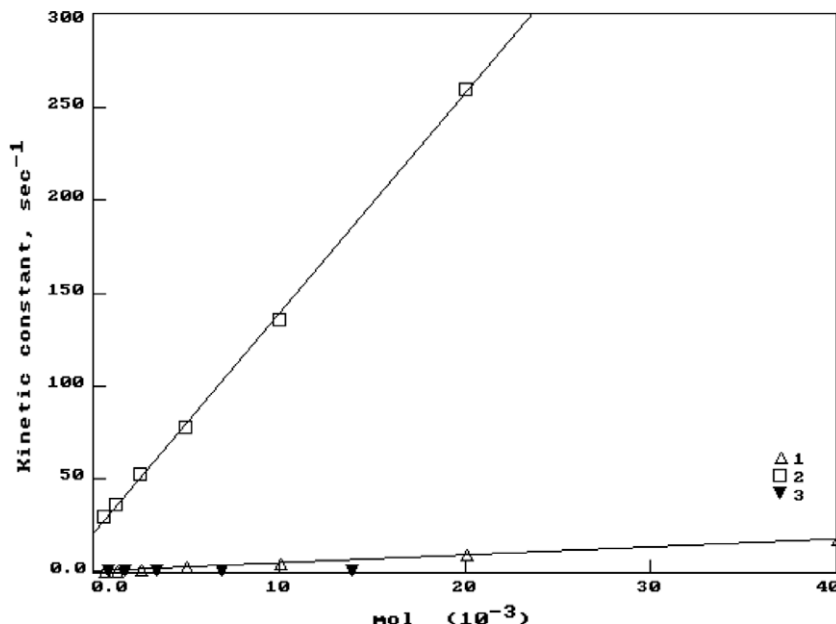


**Fig. 3.** Correlations between the pseudo first order constants and concentration for **1** (Δ) at 20 °C (Ref. [6]) and **2** (□) at 19 °C (from line-shape analysis). Independence from concentration of the first order constants (from inversion transfer) of **3** (▼) at 30 °C.

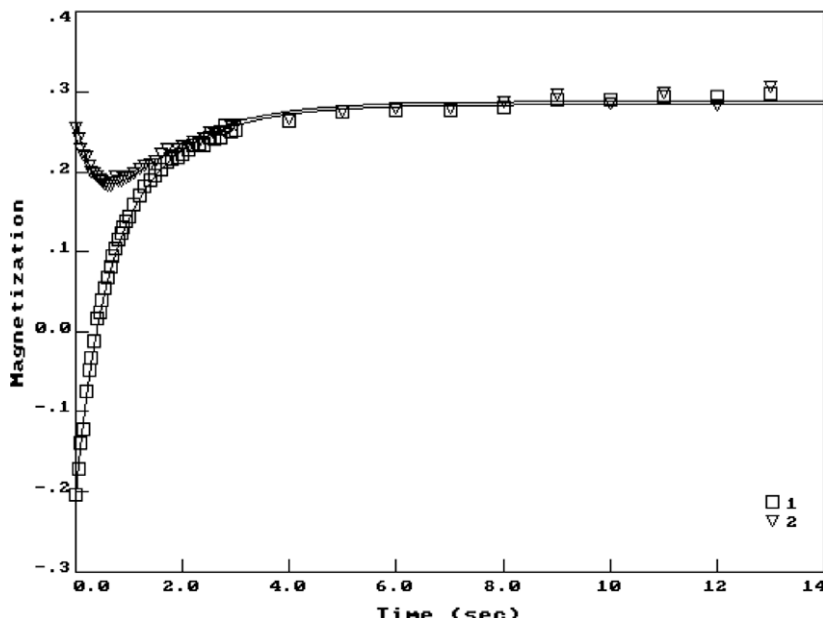


**Fig. 4.** Inversion transfer experiment for **3**, carried out at 50 °C. The high field Me singlet of tmetc (marked by □) is selectively inverted and the magnetization transferred to the low field singlet (marked by ▽). The magnetizations are taken from the peak heights in normalized spectra and the value scale is arbitrary. The data are fitted by the algorithm proposed in Ref. [14].

**Table 1**

Equilibrium (Arrhenius equation) and activation (Eyring equation) parameters for the fluxional rearrangements of **1**, **2** and **3**.

Complex	Mechanism	Monitored group	$\Delta H$ (kcal mol <sup>-1</sup> )	$\Delta H^\ddagger$ (cal mol <sup>-1</sup> K <sup>-1</sup> )	$\Delta S^\circ$	$\Delta S^\ddagger$
<b>1</b> <sup>a</sup>	Sulfur inversion <sup>c</sup>	S-CH <sub>2</sub>		11.5 ± 0.1		2.0 ± 0.3
	Olefin rotation (bimolecular <sup>c</sup> )	CH <sub>3</sub> (tmetc)		11.3 ± 0.1		1.1 ± 0.5
<b>2</b> <sup>b</sup>	Sulfur inversion <sup>c</sup>	CH <sub>3</sub> (tmetc)		10.2 ± 0.2		-12.8 ± 0.6
	Olefin rotation (bimolecular <sup>c</sup> )	S-CH <sub>2</sub>	0.77 ± 0.10	10.5 ± 0.2	-2.3 ± 0.2	2.2 ± 0.1
<b>3</b> <sup>b</sup>	Olefin rotation <sup>d</sup>	CH(fn)	0.65 ± 0.10	10.8 ± 0.2	-1.7 ± 0.1	-0.5 ± 0.1
	Olefin rotation <sup>d</sup>	CH <sub>3</sub> (tmetc)		8.1 ± 0.1		-21.4 ± 0.3
				19.2 ± 0.5		2.2 ± 0.1

<sup>a</sup> Ref.[6].

<sup>b</sup> This work.

<sup>c</sup> Line-shape simulation.

<sup>d</sup> Selective inversion transfer.

**Table 2**

Concentration dependence of the high temperature coalescence or magnetization transfer of the CH<sub>3</sub>(tmetc) signals of **1** and **3** and of the CH(fn) signals of **2**.

Species	Temperature (°C)	Concentration range (10 <sup>-3</sup> mol dm <sup>-3</sup> )	$k_2$ (slope) (mol <sup>-1</sup> dm <sup>3</sup> s <sup>-1</sup> )	$k_1$ (intercept) (s <sup>-1</sup> )	$\Delta G_\tau^\ddagger$ (kcal mol <sup>-1</sup> )
<b>1</b> <sup>a,c</sup>	20	0.625–40	(4.40 ± 0.02) × 10 <sup>2</sup>	0.40 ± 0.04	17.7
<b>2</b> <sup>b,c</sup>	19	0.625–20	(11.7 ± 0.1) × 10 <sup>3</sup>	25.6 ± 0.8	15.2
<b>3</b> <sup>b,d</sup>	30	0.87–14		Between 0.21 and 0.27 s <sup>-1</sup>	18.5–18.7

<sup>a</sup> Ref. [6].

<sup>b</sup> This work.

<sup>c</sup> Line-shape simulation.

quantitative analysis with the line-shape simulation technique. Therefore, we had to resort to the technique of selective inversion transfer.

The high field methyl resonance of tmetc was selectively inverted with a soft shaped pulse and a series of spectra was acquired with increasing delays (from 0.05 to 13 s) between the soft and the hard detection pulse. The delay dependence of the magnetizations (measured from the intensities of the signals) of the two methyl resonances was fitted by the proper algorithm [14]. One example of fitting is shown in Fig. 4.

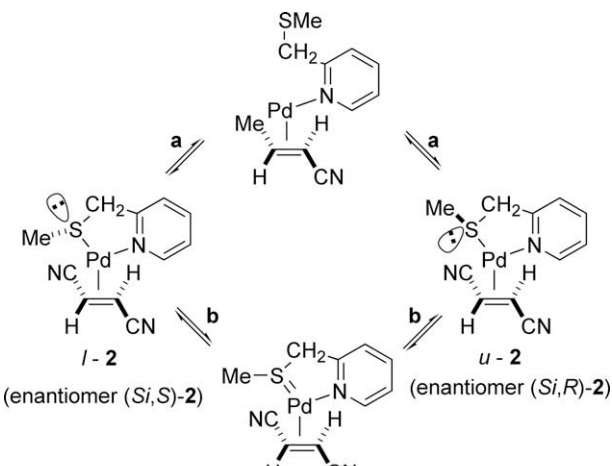
The fitting gives the rate constants for the magnetization transfer which are also the rate constants for the underlying fluxional process. The activation parameters from the Eyring plot are reported in Table 1.

For the sake of comparison, a series of experiments was carried out at a fixed temperature (30 °C) and decreasing concentrations. No dependence from concentration was noticed, as is evident from inspection of Fig. 3.

### 3. Discussion

#### 3.1. Inversion at sulfur in complexes **1** and **2**

Two mechanisms have been proposed in the literature for this process in sulfur coordinated transition-metal complexes. The first mechanism (path *a* in Scheme 1, illustrated for complex **2**), involves Pd–S bond dissociation, followed by rotation about the S-CH<sub>2</sub> bond and recombination, similar to mechanism 4 above.



This mechanism has been tentatively proposed for Pd and for other metals and always discarded [6,7,15,16].

The second mechanism (path *b* in Scheme 1) is a true inversion mechanism, implying a transition state planar at sulfur and stabilized by (p-d)  $\pi$  conjugation [16]. Because of the  $C_{2h}$  symmetry of fn, the intermediate is still asymmetric, so that the S-CH<sub>2</sub> and fn AB systems are maintained [6,7].

These arguments cannot be verified for the inversion process of complex **1**, but the conclusions can be safely extended to it on the basis of the almost negligible values of  $\Delta S^\ddagger$  and  $\Delta H^\ddagger$ . Thus mechanism *b* applies to the inversion at sulfur in complexes **1** and **2** and is also the most frequently proposed mechanism for other sulfur coordinated organometallic compounds [9,7,15,16].

The equilibrium enthalpy for **2** is small (0.65 or 0.77 kcal mol<sup>-1</sup>, depending on the monitored system) but significant. As already stated, no structural assignment of the *l*-**2** and *u*-**2** diastereoisomers was possible from low temperature NOE. The computed [10] ab initio energies (at the B3LYP/DGDZVP level) are: *l*-**2**, -5927.97423652 and *u*-**2**, -5927.97369572 hartree. The difference is 0.34 kcal mol<sup>-1</sup> favouring *l*-**2** (S-Me eclipsed with fn hydrogen) over *u*-**2** (eclipsed with fn CN). The similarity between the measured and calculated value is apparent.

### 3.2. Olefin pseudo rotation and bimolecular mechanism in complexes **1** and **2**

The detection and the quantification of propeller-like rotations in transition-metal complexes with olefins may give an estimate of the contribution of back-donation to the metal-olefin bond. To this aim, it is mandatory to unequivocally attribute the observed signal scrambling or magnetization transfer to a real rotation. As a matter of fact, we have listed 4 alternative mechanisms from literature sources, plus the one we are going to discuss in this paragraph, any of which mimicking a real propeller-like rotation mechanism. The attribution of the actual mechanism requires a closer scrutiny, such as the one we are presenting here.

The AB = BA coalescence into a singlet of the survived AB system of fn in **2**, as well as the coalescence of the residual two methyl singlets of tmec in **1** [6], are characterized by these common features: (i) the Eyring plots of the temperature dependent experiments of complexes **1** and **2** display strongly negative activation entropies (Table 1) and (ii) at a given temperature, linear correlations are found between the pseudo first order constants and complex concentration (Fig. 3 and Table 2). These points suggest the intermediation of an encounter dimer.

On the other hand, the temperature dependent experiments of inversion transfer performed on complex **3** give a Eyring plots with an absolute activation entropy well below the threshold of 5 cal mol<sup>-1</sup> K<sup>-1</sup> (Table 1), while no concentration dependence could be found (Fig. 3 and Table 2). It may then be argued that the formation of the dimer is induced by the most relevant feature that differentiates N-SMe from *N,N'*-4-anisyl, i.e. the presence of the free electron pair at sulfur.

The dimeric complex, either an intermediate or a transition state, must account for the scrambling of the chemical environments of the fn protons but also for the persistency of those of the S-CH<sub>2</sub> protons. As a matter of fact, if the enantiotopic faces of the olefin fn are not taken into account only two different encounter dimers can be drawn in the event that the two molecules will approach remaining on parallel planes (those defined by the ancillary ligand, dimers **d1** and **d2** in Fig. 5).

Similar bridging complexes are not unusual in the chemistry of palladium as is documented in the crystal structures of some dimeric complexes between Pd planar units (with carbon and nitrogen or with oxygen, rather than sulfur and nitrogen, bridges) ([17] and references therein). Among all, only the collapse of the dimer **d1** allows the exchange between the ligand coordinating atoms and the consequent olefin pseudo rotation independently of the olefin enantioface (Fig. 5). In this case, the AB system related to the olefin protons collapses but, as the observed phenomenon indicates, the S-CH<sub>2</sub> protons still remain diastereotopic since the molecular chirality induced by the olefin enantiotopic face is not changing at all.

### 3.3. Olefin rotation in complexes **1**, **2** and **3**

The plots for **1** and **2** of the pseudo first-order constants versus concentration (Fig. 2) display intercepts (Table 2) which are statistically significant and positive, compatible with a monomolecular process. The activation entropy from the Eyring plot for **3** is again indicative of a monomolecular process. Only mechanisms 1 and 4 in the above list are rigorously monomolecular. We favour mechanism 1, describing a true propeller-like rotation since the *k*<sub>1</sub> kinetic constants in Table 2 are more dependent on the nature of the olefin than on that of the ancillary ligand (Table 2) [18].

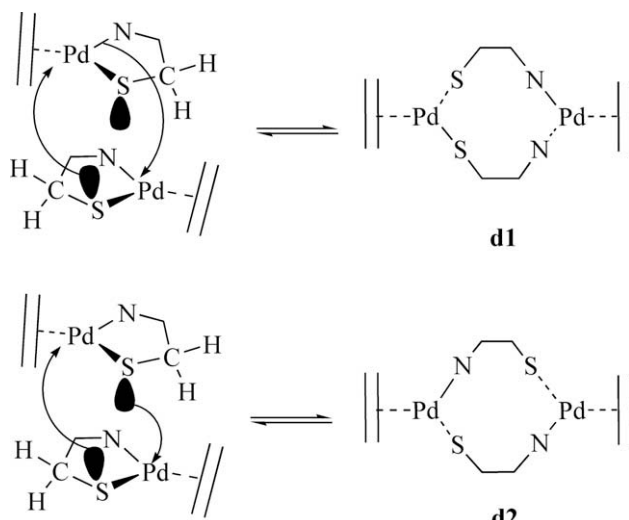


**Fig. 5.** Bimolecular intermediates derived from different approach of two molecules of Pd( $\eta^2$ -olefin) pyridylthioether derivatives. The collapse of the **d1** intermediate induces the exchange between the ancillary ligand coordinating atoms (olefin pseudo rotation).

Thus, the kinetic parameters for **3** in Table 1 and the kinetic constants in Table 2, which have been obtained with due accuracy [12], are indicative of the back-donation contribution to the olefin-metal bond. More rigorously, they reveal the difference between the strong back-donation in the planar ground state (from the relevant interaction of the empty  $\pi^*$  orbital of the olefin with the occupied, symmetrically correct,  $\delta$  orbital of the d<sup>10</sup> Pd(L-L') moiety, which is high lying) and the smaller back-donation in the perpendicular transition state (where the interaction is with a  $\delta$  orbital with different symmetry, albeit rather low lying) [19].

#### 4. Conclusion

The detailed <sup>1</sup>H NMR investigation carried out in this study allows the univocal interpretation of the mechanism governing the fluxional behaviour of the low-valent palladium alkene derivatives. On the basis of symmetry and energy considerations the sulfur absolute configuration and the olefin rotation were somewhat established, while the mechanism involving the olefin pseudo rotation in pyridylthioether palladium alkene derivatives, promoted by a low energy bimolecular rearrangement triggered by the sulfur lone pair, was unambiguously confirmed.

#### 5. Experimental

The <sup>1</sup>H NMR experiments were carried out by means of a VARIAN 400 Unity spectrometer in CD<sub>2</sub>Cl<sub>2</sub> or CDCl<sub>3</sub> as solvent. The uncertainty in the temperature measurement is estimated at  $\pm 1$  K.

The iterative fitting of the ensuing spectra by the DNMR5 program [11] gives the kinetic and the equilibrium constants together with the corresponding errors. The thermodynamic parameters were computed by linear regression according to Arrhenius or Eyring equations.

The complexes [Pd( $\eta^2$ -tmetc)(N-SMe)] (**1**), [Pd( $\eta^2$ -fn)(N-SMe)] (**2**) [7] and [Pd( $\eta^2$ -tmetc)(N-N'-4-anisyl)] (**3**) [8] were synthesized and characterized according to published methods.

#### Appendix A. Supplementary material

Supplementary data associated with this article can be found, in the online version, at doi:10.1016/j.ica.2008.12.010.

#### References

- [1] R. Cramer, G.B. Kline, J.D. Roberts, J. Am. Chem. Soc. 91 (1969) 2519.
- [2] F.P. Fanizzi, F.P. Intini, L. Maresca, G. Natile, M. Lanfranchi, A. Tiripicchio, J. Chem. Soc., Dalton Trans. (1991) 1007.
- [3] R. van Asselt, C.J. Elsevier, W.J.J. Smeets, A.L. Speck, Inorg. Chem. 33 (1994) 1521.
- [4] (a) R. Fernandez Galan, F.A. Jalon, B.R. Manzano, J. Rodriguez de la Fuente, M. Vrahami, B. Jedlika, W. Weissenstein, G. Jogi, Organometallics 16 (1997) 3758;  
 (b) F. Gomez de la Torre, F.A. Jalon, A. Lopez Agenjo, T. Sturm, W. Weissenstein, M.M. Ripoll, Organometallics 17 (1998) 4634.
- [5] F.A. Jalon, B.R. Manzano, F. Gomez de la Torre, A. Lopez Agenjo, A.M. Rodriguez, W. Weissenstein, T. Sturm, J. Mahia, M. Maestro, J. Chem. Soc., Dalton Trans. (2001) 2417.
- [6] L. Canovese, V. Lucchini, C. Santo, F. Visentin, A. Zambon, J. Organomet. Chem. 642 (2002) 58.
- [7] L. Canovese, F. Visentin, G. Chessa, P. Uguagliati, A. Dolmella, J. Organomet. Chem. 601 (2000) 1.
- [8] L. Canovese, F. Visentin, P. Uguagliati, B. Crociani, J. Chem. Soc., Dalton Trans. (1996) 1921.
- [9] The enantiotopic faces of the Pd-bound N-SMe are recognized on the basis of the Pd > S > N priority, and are named *R* and *S*. For the sake of distinction, the enantiotopic faces of fn are named *Re* and *Si*. As an obvious extension, the diastereoisomers with S-Me pointing toward the *R* or *S* face are also named *R* or *S*, respectively.
- [10] Geometry optimizations at the RB3LYP/DGDVZP level: M.J. Frisch, G.W. Trucks, H.B. Schlegel, G.E. Scuseria, M.A. Robb, J.R. Cheeseman, V.G. Zakrzewski, J.A. Montgomery Jr., R.E. Stratmann, J.C. Burant, S. Dapprich, J.M. Millam, A.D. Daniels, K.N. Kudin, M.C. Strain, O. Farkas, J. Tomasi, V. Barone, M. Cossi, R. Cammi, B. Mennucci, C. Pomelli, C. Adamo, S. Clifford, J. Ochterski, G.A. Petersson, P.Y. Ayala, Q. Cui, K. Morokuma, D.K. Malick, A.D. Rabuck, K. Raghavachari, J.B. Foresman, J. Cioslowski, J.V. Ortiz, B.B. Stefanov, G. Liu, A. Liashenko, P. Piskorz, I. Komaromi, R. Gomperts, R.L. Martin, D.J. Fox, T. Keith, M.A. Al-Laham, C.Y. Peng, A. Nanayakkara, C. Gonzalez, M. Challacombe, P.M.W. Gill, B.G. Johnson, W. Chen, M.W. Wong, J.L. Andres, M. Head-Gordon, E.S. Replogle, J.A. Pople, GAUSSIAN 98, Revision 5.4, GAUSSIAN, Inc., Pittsburgh, PA, 1998.
- [11] (a) D.S. Stephenson, G. Binsch, J. Magn. Reson. 32 (1978) 145;  
 (b) D.S. Stephenson, G. Binsch, DNMR5, QCPE 365. Modified by LeMaster, C.B., LeMaster, C.L., True, N.S. QCMP 059.
- [12] Quantitative evaluations of the olefin rotation in Pd complexes are not frequent (see Refs. [1–4]), and are always presented as kinetic constants or  $\Delta G^\ddagger$  activation free energies, calculated at the coalescence temperature with standard formulas. These evaluations are however biased by the fact that the  $\Delta v$  values, present in these formulas, are taken from ‘frozen’ low temperature spectra. This inconsistency was pointed out and briefly commented in Ref. [1].
- [13] A dimeric intermediate was invoked as a rationale of the second order dependence found in another process monitored by NMR: R. van Belzen, R.A. Klein, H. Kooijman, N. Veldman, A.L. Spek, C.J. Elsevier, Organometallics 17 (1998) 1812.
- [14] J.R. Alger, J.H. Prestgard, J. Magn. Reson. 27 (1977) 137.
- [15] (a) D.D. Gummin, E.M.A. Ratilla, N.M. Kostic, Inorg. Chem. 25 (1986) 2429;  
 (b) M. Oki, Pure Appl. Chem. 61 (1989) 699;  
 (c) S.S. Oster, W.D. Jones, Inorg. Chim. Acta 357 (2004) 1836.
- [16] (a) E.W. Abel, E.W. Raeeow, G.W. Orrell, K.G.W. Sik, J. Chem. Soc., Dalton Trans. (1977) 42;  
 (b) X. Shan, J.H. Espenson, Organometallics 22 (2003) 1250.
- [17] (a) L. Canovese, F. Visentin, C. Santo, C. Levi, A. Dolmella, Organometallics 26 (2007) 5590;  
 (b) M.H. Johansson, A. Oskarsson, Acta Crystallogr. C 57 (2001) 1265.
- [18] The fluxional behaviour of some Pd(olefin) complexes with ancillary ligands that are permanently dissymmetric (Ref. [4]) and of some square tetragonal Pd(bipyridine) complexes: J.G.P. Delis, P.G. Aubel, K. Vrieze, P.W.N.M. van Leeuwen, N. Veldman, A.L. Spek, F.J.R. van Neer, Organometallics 16 (1997) 2948 (requires the Pd-N disconnection).
- [19] See Fig. 4 in: T.A. Albright, R. Hoffmann, J.C. Thibeault, D.L. Thorn, J. Am. Chem. Soc. 101 (1979) 3801.